arXiv:1603.03624v1 [cs.SY] 11 Mar 2016

Consensus algorithms and plug-and-play control for current sharing in DC microgrids

Michele Tucci*[1], Lexuan Meng†[2], Josep M. Guerrero‡ [2], and Giancarlo Ferrari-Trecate§ [1]

[1] *Dipartimento di Ingegneria Industriale e dell'Informazione, Università degli Studi di Pavia*

[2] *Institute of Energy Technology, Aalborg University*

Technical Report
March, 2016

Abstract

In this paper, we propose a secondary consensus-based control layer for current sharing and voltage balancing in DC microGrids (mGs). Differently from existing approaches based on droop control, we assume decentralized Plug-and-Play (PnP) controllers at the primary level as they provide voltage stabilization and their design complexity is independent of the mG size. We analyze the behavior of the closed-loop mG by approximating local primary control loops with either unitary gains or first-order transfer functions. Besides proving stability, current sharing and voltage balancing in the asymptotic régime, we describe how to design secondary controllers in a PnP fashion when distributed generation units are added or removed. Theoretical results are complemented by simulations using a 5-DGUs mG implemented in Simulink/PLECS.

Keywords: DC microgrid, secondary control, current sharing, voltage balancing, plug-and-play.

*Electronic address: michele.tucci02@universitadipavia.it; Corresponding author
†Electronic address: lme@et.aau.dk
‡Electronic address: joz@et.aau.dk
§Electronic address: giancarlo.ferrari@unipv.it

1 Introduction

Power generation and distribution is deeply changing due to the increasing diffusion of renewable energy sources, advances in energy storage, and active participation of consumers to the energy market [1]. This shift of paradigm motivated the development of migroGrids (mGs), commonly recognized as small-scale power system integrating Distributed Generation Units (DGUs), storage devices and loads. In addition, mGs can operate either connected to the main grid or in islanded mode [2, 3]. Since AC power generation is the standard for commercial, residential and industrial utilization, several studies focused on AC mGs [4, 5, 6, 7]. However, nowadays, DC energy systems are gaining interest [8, 9] because of the increasing number of DC loads, the availability of efficient converters, and the need of interfacing DC energy sources and batteries with minimal power losses. In particular, DC mGs are becoming more and more popular in several application domains, such as avionics, automotive, marine and residential systems. A key feature of DC mGs is that they can be coupled to the main grid only through AC-DC converters. These devices always limit the power transfer and, therefore, DC mGs can be thought as operating in islanded mode only. The basic issues in control of DC mGs are voltage stabilization [8, 10] and current sharing, the latter meaning that DGUs must compensate load currents proportionally to their ratings and independently of the mG topology and line impedances. An additional goal is voltage balancing, i.e. to keep the average output voltage of DGUs close to a prescribed level.

To realize these objectives, hierarchical control structures have been proposed. In the primary layer, current sharing regulation is usually implemented on top of local controllers comprising voltage and current loops. While centralized controllers can ensure voltage stabilization and accurate current sharing [11], the computational and communication burden of these architectures increases with the mG size. Moreover, a single-point-of-failure in the central unit may cause the malfunction of the whole system [12, 13]. For these reasons, decentralized and distributed regulators, such as droop controllers [9], are preferred. Droop control is a communication-less approach, but it might cause deviations of voltages from reference values. For solving this problem, droop controllers are often complemented with consensus algorithms [14] forming a secondary control layer [15, 16, 12, 17].

In order to stabilize mGs with general topologies, the design of droop and consensus controllers is often done in a centralized fashion, i.e. exploiting knowledge about all DGUs and line models [14, 15, 12, 17]. These design approaches, however, become prohibitive when the mG size grows. Furthermore, in order to preserve stability, the plugging-in or out of DGUs might require the update of all local controllers in the mG. This motivated the development of scalable design procedures for local controllers [10, 16]. In [16] the authors propose primary droop regulators tightly coupled with secondary consensus filters for guaranteeing voltage stability and current sharing. For analysis purposes, inner voltage and current loops are simplified as unitary gains. For this approximation to hold, the interconnection of DGUs, equipped with inner loops only, must be asymptotically stable. In order to guarantee voltage stability, in [10] inner loops and droop controllers have been replaced by a new class of primary controllers, termed Plug-and-Play (PnP). Local PnP regulators also allow to tune the bandwidth of controlled DGUs through the use of prefilters. Furthermore, when a DGU wants to join the network, the possibility of designing PnP regulators for the DGU and its future neighbors can be automatically checked by solving local optimization problems exploiting information only about individual DGUs and the lines connected to them. In this way, the plug-in of DGUs is automatically denied, if dangerous for mG stability.

The goal of this paper is to enhance PnP controllers with secondary regulators for achieving current sharing and voltage balancing. Similarly to [12, 16, 15, 17], we exploit consensus filters requiring DGUs to communicate in real-time over a network with arbitrary, yet connected, topology. We rigorously analyze the behavior of the closed-loop mG by approximating primary control loops with either unit gains (as in [16]) or first-order transfer functions.

Current sharing and voltage balancing properties, are also demonstrated in simulation using a 5-DGUs mG implemented in Simulink/PLECS [18], accounting for the non-idealities of real converters and lines.

Notation and basic definitions. The cardinality of the finite set S will be denoted with $|S|$.

A weighted graph is a directed graph $\mathcal{G} = (\mathcal{V}, \mathcal{E}, W)$ defined by the set of nodes $\mathcal{V} = \{1, \dots, n\}$, the set of edges $\mathcal{E} \subseteq \mathcal{V} \times \mathcal{V}$ and the diagonal matrix $W \in \mathbb{R}^{|\mathcal{E}|\times|\mathcal{E}|}$ collecting on its diagonal the weights w_i associated to edges $e_i \in \mathcal{E}$ (i.e. $W_{ii} = w_i$). The set of neighbors of node $i \in \mathcal{V}$ is $\mathcal{N}_i = \{j : (i,j) \in \mathcal{E} \text{ or } (j,i) \in \mathcal{E}\}$. $Q(\mathcal{G}) \in \mathbb{R}^{|\mathcal{V}|\times|\mathcal{E}|}$ is the incidence matrix of $\mathcal{G}$ [19]. The Laplacian matrix of $\mathcal{G}$ is $\mathcal{L}(\mathcal{G}) = Q(\mathcal{G})WQ(\mathcal{G})^T$, independently of the orientation of edges.

The eigenvalues of a square matrix $\mathcal{A}$ of dimension $n \times n$ are denoted with $\lambda_i(\mathcal{A})$, $i = 1, \dots, n$.

An Hermitian matrix $\mathcal{A} \in \mathbb{C}^{n\times n}$ is positive (resp. negative) definite if $x^\star \mathcal{A} x$ is *real* and positive (resp. negative) for all non-zero column vectors $x \in \mathbb{C}^{n\times n}$ ($x^\star$ denotes the conjugate transpose of x). A positive (resp. negative) semi-definite Hermitian matrix is defined in the same way, except that the expression $x^* \mathcal{A} x$ is required to be always non-negative (resp. non-positive). If $\mathcal{A} \in \mathbb{R}^{n\times n}$, the above definitions can be similarly reformulated in the real sense, by just considering non-zero column vector $x \in \mathbb{R}^n$ and replacing $x^\star$ with x^T. Moreover, if a real matrix is also symmetric, we have consistency between real and complex definitions [20].

The $n \times 1$ vector of ones (resp. zeros) is denoted as $\mathbf{1}_n$ (resp. $\mathbf{0}_n$).

The average of a vector $v \in \mathbb{R}^n$ is $\langle v \rangle = \frac{1}{n}\sum_i^n v_i$. We denote with H^1 the subspace composed by all vectors with zero average [21, 22] i.e. $H^1 = \{v \in \mathbb{R}^n : \langle v \rangle = 0\}$. The space orthogonal to H^1 is $H^1_\perp$. It holds $H^1_\perp = \{\alpha \mathbf{1}_n,\ \alpha \in \mathbb{R}\}$ and $\dim(H^1_\perp) = 1$. Moreover, the decomposition $\mathbb{R}^n = H^1 \oplus H^1_\perp$ is direct [23], i.e each vector $v \in \mathbb{R}^n$ can always be written in a unique way as

$$v = \hat{v} + \bar{v} \quad \text{with } \hat{v} \in H^1 \text{ and } \bar{v} \in H^1_\perp. \tag{1}$$

Consider the matrix $A \in \mathbb{R}^{n\times n}$. With the notation $A(H^1|H^1)$ we indicate the linear map $A : H^1 \to H^1$ (i.e. the restriction of the map $A : \mathbb{R}^n \to \mathbb{R}^n$ to the subspace H^1). For a subspace $\mathcal{V} \subset \mathbb{R}^n$, we denote with $P_{\mathcal{V}}(v)$ the projection of $v \in \mathbb{R}^n$ on $\mathcal{V}$.

The subspace $\mathcal{V} \subseteq \mathbb{R}^n$ is said to be *A-invariant* if $v \in \mathcal{V} \Rightarrow Av \in \mathcal{V}$.

The subspace $\mathcal{V} \subseteq \mathbb{R}^n$ is *invariant* for the system $\dot{x} = Ax + Bu$ and $\mathcal{U} \subseteq \mathbb{R}^m$ if

$$x(0) \in \mathcal{V} \Rightarrow x(t) \in \mathcal{V},\ \forall t \geq 0,\ \forall u(t) \in \mathcal{U}.$$

Preliminaries on Laplacian matrices. Laplacian matrices have key properties summarized in the next Proposition.

Proposition 1. *For a connected graph $\mathcal{G}$ with weights $w_i > 0$, $A = \mathcal{L}(\mathcal{G}) \in \mathbb{R}^{n\times n}$ has the following properties:*

(i) it has non positive off-diagonal elements;

(ii) $\lambda_1(A) \geq \cdots \geq \lambda_{n-1}(A) \geq 0 = \lambda_n$*;*

(iii) $\mathrm{Ker}(A) = H^1_\perp$ *and* $\mathrm{Range}(A) = H^1$*;*

(iv) $A(H^1|H^1)$ is invertible.

Proof. Points (i)-(iii) are shown, e.g. in [24, 25]. Point (iv) has been shown in [21] with the framework of partial difference equations. Next, we provide a proof based on linear algebra only. We start noticing that the linear map $A(H^1|H^1)$ invertible if it is surjective and injective [26]. First, we show the surjectivity of A on H^1. By construction, $\mathrm{rank}(A) = n - 1$ because

$$\mathrm{rank}(A) = \dim(\mathrm{Range}(A)) = \dim(\mathbb{R}^n) - \dim(H^1_\perp) = n - 1.$$

Moreover, since A is symmetric, each column of A has zero sum and hence is a vector in H^1. Since $\mathrm{Range}(A)$ is the column span, then $\mathrm{Range}(A) \subset H^1$. Since $\dim(H^1) = n - 1$, one obtains $\mathrm{Range}(A) = H^1$. This proves that the map $A(H^1|H^1)$ is surjective.
Next, we prove that $A(H^1|H^1)$ is also injective. By definition, this holds if

$$\forall b \in H^1 \quad \forall x, y \in H^1 \quad (Ax = b \text{ and } Ay = b) \Rightarrow x = y.$$

Now, $Ax = Ay = b$ implies that $A(x - y) = 0$. It means that $x - y \in \mathrm{Ker}(A)$, therefore $\exists \alpha \in \mathbb{R}$ such that $x - y = \alpha \mathbf{1}_n$. However, since $x - y \in H^1$, $x - y = \alpha \mathbf{1}_n$ is verified only for $\alpha = 0$; this leads to $x = y$. □

2 Plug-and-play primary voltage control

2.1 DGU electrical model

As in [10], we consider a DC mG composed of N DGUs. For the sake of clarity, the electrical scheme of the i-th DGU is shown in Figure 1. In each DGU, the generic renewable resource is modeled as a DC voltage source and a Buck converter is used to supply a local load connected to the Point of Common Coupling (PCC) through an RL filter. As in [27], an averaging technique is adopted for modeling the Buck converter so as to neglect high frequency switching dynamics. Furthermore, we assume that loads I_{Li} are unknown and treated as current disturbances [28, 10]. The controlled variable is the voltage at each PCC. From Figure 1, by applying Kirchoff's voltage and current laws and exploiting Quasi Stationary Line (QSL) approximation of power lines [29], we obtain the following model of DGU i[1]

$$\text{DGU } i: \begin{cases} \dfrac{dV_i}{dt} = \dfrac{1}{C_{ti}} I_{ti} + \displaystyle\sum_{j \in \mathcal{N}_i} \left(\frac{V_j}{C_{ti} R_{ij}} - \frac{V_i}{C_{ti} R_{ij}} \right) - \frac{1}{C_{ti}} I_{Li} \\ \dfrac{dI_{ti}}{dt} = -\dfrac{1}{L_{ti}} V_i - \dfrac{R_{ti}}{L_{ti}} I_{ti} + \dfrac{1}{L_{ti}} V_{ti} \end{cases} \tag{2}$$

where inputs (V_{ti}, I_{Li}) and $V_j \in \mathcal{N}_i$, states (V_i, I_{ti}), and electrical parameters R_{ti}, C_{ti}, L_{ti} and R_{ij} are shown in Figure 1. In particular, V_j is the voltage at the PCC of each neighboring DGU $j \in \mathcal{N}_i$.

Remark 1. *From Figure 1, we assume a "load-connected" topology, meaning that load currents are located at the PCC of each DGU. This restriction on the mG topology is, however, mild. Indeed, as shown in [16, 30, 31], arbitrary interconnections of DGU and load nodes can be always mapped into load-connected mGs through a network reduction method known as Kron reduction.*

2.2 Plug-and-play design

In this Section, we briefly summarize the PnP scalable approach in [10] for designing primary decentralized controllers guaranteeing voltage stability in DC mGs. Local regulator $\mathcal{C}_i$ of DGU i exploits measurements of V_i and I_{ti} to compute the command V_{ti} of the i-th Buck converter and make V_i track a reference signal $V_{ref,i}$ (see the scheme in Figure 1). Each controller is composed by a vector matrix gain K_i and an integral action is present for zeroing the voltage tracking error. The decentralized design of these vector gains is the core of PnP controller synthesis. More specifically, as shown in [10]: (i) the design of K_i requires only knowledge of the dynamics of DGU i and the parameters of power lines connecting it to its neighbors, (ii) K_i is automatically computed solving a Linear Matrix Inequality (LMI) problem.

For modeling the interaction of multiple DGUs, we represent the mG with a directed graph $\mathcal{G}_{el} = (\mathcal{V}_{el}, \mathcal{E}_{el}, W)$ (see e.g. Figure 2), where (i) each node is a DGU with local PnP controller and local current load, (ii) edges (i, j) are power lines, and weights are the corresponding conductances[2], $\frac{1}{R_{ij}}$, (iii) we set $N = |\mathcal{V}_{el}|$ and $M = |\mathcal{E}_{el}|$. Next, we show how to handle plugging -in/-out of DGUs while preserving the stability of the mG. Whenever a DGU (say DGU i) wants to join the network (e.g. DGU 6 in Figure 2), it sends a plug-in request to its future neighbors, i.e. DGUs $j \in \mathcal{N}_i$ (e.g. DGUs 1 and 5 in Figure 2). Then, DGU i solves the LMI problem (15) in [10]. If the optimization problem is feasible, it returns a controller $\mathcal{C}_i$ (i.e. a vector gain K_i) along with a local separable Lyapunov function that can be used for certifying stability of the whole mG. Since also DGUs $j \in \mathcal{N}_i$ will have a new neighbor, they might need to update their controller $\mathcal{C}_j$ by tacking into account the impedance of the new line ji. If LMI constraints of problem (15) in [10] for DGU j are still fulfilled, no update is necessary. Otherwise, DGU j solves an LMI problem analogous to the one solved by DGU i. If one of the above LMI problems is unfeasible, plug-in of DGU i is

[1] For the detailed DGU model derivation, we defer the reader to [10].

[2] Line inductances L_{ij} are neglected as we assume QSL approximations [29].

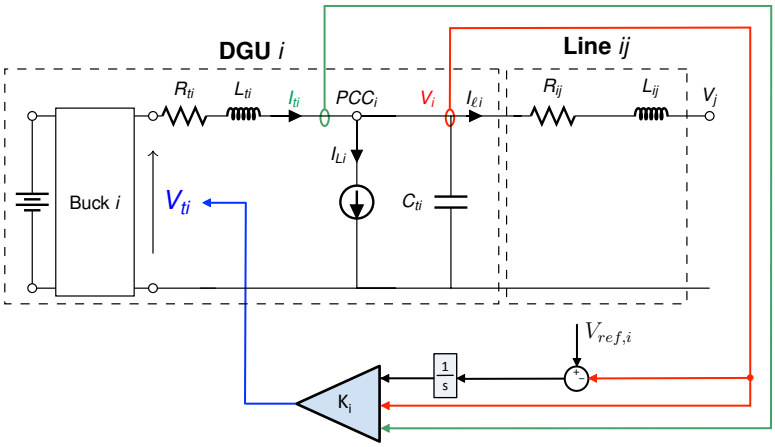

Figure 1: Electrical scheme of DGU i and local PnP voltage controller.

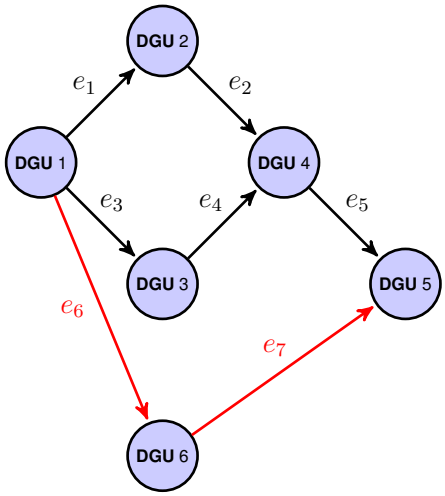

Figure 2: Graph representation of an mG composed of 5 DGUs (in black) and plug-in of DGU 6 (in red).

denied. Otherwise, DGU i can be connected and stability of the whole mG can be certified using the sum of the computed local Lyapunov functions. Unplugging of a DGU (say DGU m) follows a similar procedure: as line mk will be disconnected from the corresponding DGU k, all controllers $\mathcal{C}_k$, $k \in \mathcal{N}_m$ must be successfully redesigned before allowing the disconnection.

Remark 2. *Local PnP controllers can be enhanced with pre-filters so as to shape in a desired way the transfer function $G_i(s)$ between voltages $V_{ref,i}$ and V_i represented in Figure 1. Therefore, it is possible to identify a range of frequencies in which $G_i(s)$ can be approximate as an unitary gain or a first-order system. In particular, the presence of an integrator in each local control scheme allows the voltage V_i at the PCC to track constant references when the disturbances (i.e. load currents I_{Li}) are constant [10].*

3 Secondary control based on consensus algorithms

PnP local regulators form a primary control layer capable to regulate the voltage at each PCC while guaranteeing stability of the overall mG. However, they do not to ensure current sharing

and voltage balancing, defined as follows.

Definition 1. *Current sharing is achieved if the overall load current is equally shared among DGUs, i.e.*

$$I_{ti} = \langle \mathbf{I_L} \rangle \quad i = 1, \ldots, N, \tag{3}$$

where $\mathbf{I_L} = [I_{L1}, I_{L2}, \ldots, I_{LN}]^T$ *is the vector of local load currents.*

Assumption 1. *Voltage references are identical for all DGUs, i.e.* $V_{ref,i} = V_{ref}$, $\forall i \in \mathcal{V}_{el}$.

Definition 2. *Under Assumption 1, voltage balancing is achieved if*

$$\langle \mathbf{V} \rangle = V_{ref}. \tag{4}$$

where vector $\mathbf{V} = [V_1, V_2, \ldots, V_N]^T$ *collects the PCC voltages.*

We highlight that current sharing is desirable in order to avoid situations in which some DGUs are not able to supply local loads, thus requiring power from other DGUs. A safe way to perform this operation is to make DGUs proportionally share their load current, according, for instance, to their generation capacity. This can be obtained by ensuring (3) while measuring the currents in per-unit (p.u.), with base currents equal to the current ratings of Buck converters.

Even if current sharing holds, the voltages at PCCs may have deviation from the nominal value. If not well controlled, overall voltage fault may happen to some PCCs. Accordingly, another objective is to ensure the average voltage value among all PCCs is equal to the nominal value (V_{ref}).

In order to guarantee current sharing and voltage balancing, we enhance primary PnP controllers with a consensus-based secondary control layer. In general, consensus algorithms can be used to achieve information sharing and coordination among agents. In our case, as shown in Figure 3, a basic consensus scheme with continuous-time integrators [32], adjusts the voltage references for each PnP regulator while considering the output current differences among DGUs, i.e.

$$\Delta \dot{V}_i(t) = k_{I,i} \sum_{j=1, j\neq i}^{N} a_{ij}(I_{ti}(t) - I_{tj}(t)), \tag{5}$$

where $a_{ij} = 1$ if DGUs i and j are connected by a communication link and $a_{ij} = 0$ otherwise.

Assumption 2. *Integral coefficients* $k_{I,i}$ *are equal for all the DGUs (i.e.* $k_{I,i} = k_I$, $i = 1, \ldots, N$*).*

We assume bidirectional communication, i.e. $a_{ij} = a_{ji}$. Weights $a_{ij} \neq 0$ induce a communication graph $\mathcal{G}_c = (\mathcal{V}_{el}, \mathcal{E}_c, W_c)$ with unit weights, whose topology can be different from that of $\mathcal{G}_{el}$. More precisely, we assume that DGUs i and j communicate if $a_{ij} \neq 0$, i.e. $(i, j) \in \mathcal{E}_c \iff a_{ij} \neq 0$. From now on, we will make the following standing assumption.

Assumption 3. *The graph* $\mathcal{G}_{el}$ *is weakly connected and the graph* $\mathcal{G}_c$ *is connected.*

From a system point of view, the collective dynamics of the group of DGUs following (5) can be expressed as

$$\dot{\mathbf{\Delta V}} = -\underbrace{\mathcal{K}_I L}_{\mathbb{L}} \mathbf{I_t}, \tag{6}$$

where $\mathbf{\Delta V} = [\Delta V_1, \ldots, \Delta V_N]^T = \mathbf{V} - \mathbf{V_{ref}}$, $\mathbf{V_{ref}} = [V_{ref,1}, V_{ref,2}, \ldots, V_{ref,N}]^T$, $\mathbf{I_t} = [I_{t1}, I_{t2}, \ldots, I_{tN}]^T$ collects the converter output currents, $\mathcal{K}_I = \text{diag}(k_I, \ldots, k_I) \in \mathbb{R}^{N\times N}$ and $L = \mathcal{L}(\mathcal{G}_c)$. Furthermore, my means of Assumption 2, $\mathbb{L}$ is a Laplacian matrix.

4 Modeling and analysis of the complete system

The hierarchical scheme of DGU i equipped with primary and secondary control loops is shown in Figure 3. In order to assess the behavior of the overall closed-loop mG, we perform two separate analysis where each PnP-controlled DGU is approximated either as an unit-gain or as a first-order transfer function.

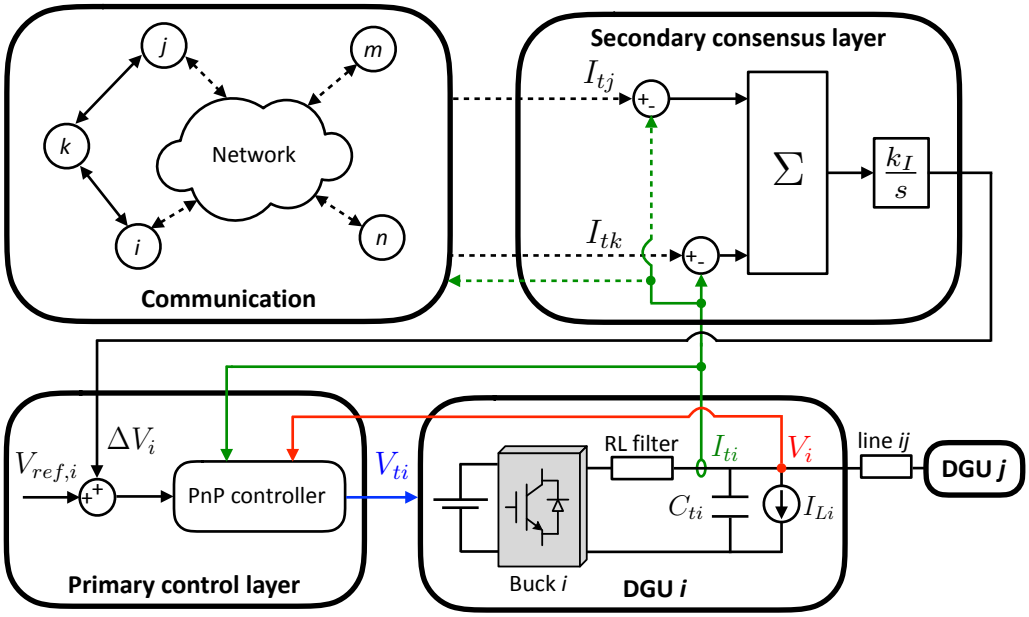

Figure 3: Complete hierarchical control scheme of DGU i.

4.1 Unit-gain approximation of PnP-controlled DGUs

By approximating primary PnP loops with ideal unitary gains, we have the relations $V_i = V_{ref,i} + \Delta V_i$, $\forall i \in \mathcal{V}_{el}$. This approximation is reasonable at low frequencies (see Remark 2). Furthermore, it allows us to develop, in a simple setting, methods and tools that will be also used in the more complex case considered in Section 4.2.

The resulting hierarchical control scheme is shown in Figure 4. In order to derive the dynamics of the overall mG as a function of the inputs $\mathbf{I_L}$ and $\mathbf{V_{ref}}$, we write relations among variables in Figure 4a-4b. Hence, we have (6) and

$$\mathbf{V} = \mathbf{\Delta V} + \mathbf{V_{ref}}. \tag{7}$$

From basic circuit theory, the relation between the vector of voltages $\mathbf{V}$ and the vector of line currents $\mathbf{I}_\ell = [I_{\ell 1}, \dots, I_{\ell M}]^T$ is

$$\mathbf{I}_\ell = -WB^T\mathbf{V} \tag{8}$$

where W is the weight matrix of $\mathcal{G}_{el}$ and $B = Q(\mathcal{G}_{el})$ is the incidence matrix of the mG. From Figure 4, we also get

$$\mathbf{I_t} = \mathbf{I_L} - B\mathbf{I}_\ell \tag{9}$$

and, merging equations (6)-(9), we finally obtain

$$\begin{aligned} \dot{\mathbf{\Delta V}} &= -\mathbb{L}\underbrace{BWB^T}_{\mathbb{M}}\mathbf{\Delta V} - \mathbb{L}\mathbf{I_L} - \mathbb{L}\underbrace{BWB^T}_{\mathbb{M}}\mathbf{V_{ref}} \\ &= -\mathbb{Q}\mathbf{\Delta V} - \mathbb{L}\mathbf{I_L} - \mathbb{Q}\mathbf{V_{ref}} \end{aligned} \tag{10}$$

where matrix $\mathbb{M} = \mathcal{L}(\mathcal{G}_{el}) = BWB^T$ is the Laplacian matrix of the electrical network and $\mathbb{Q} = \mathbb{L}\mathbb{M}$. The matrix $\mathbb{Q}$ can fail to have all properties typical of Laplacian matrices. For instance, the product of two Laplacian matrices might be not symmetric and might have positive off-diagonal entries, even though weights of $\mathcal{G}_{el}$ and $\mathcal{G}_c$ are positive. However, $\mathbb{Q}$ has several features in common with Laplacian matrices, as shown in the next Proposition.

Proposition 2. *The matrix $\mathbb{Q}$ has the following properties:*

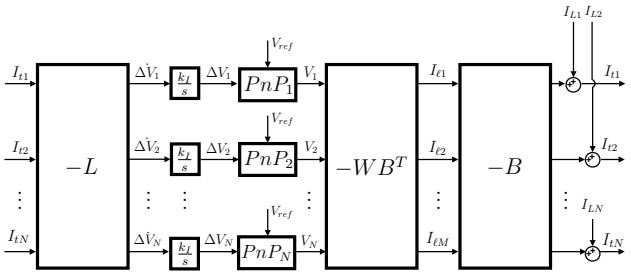

(a) Hierarchical control scheme.

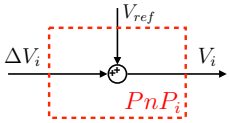

(b) i-th ideal primary PnP loop.

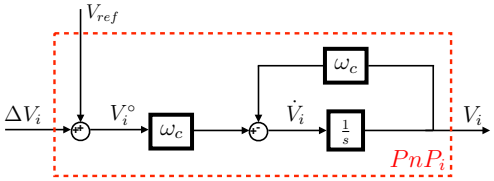

(c) First-order approximation of the i-th PnP loop.

Figure 4: Hierarchical control scheme and primary PnP loops approximations.

(i) $\mathrm{Ker}(\mathbb{Q}) = H^1_\perp$;

(ii) $\mathrm{Range}(\mathbb{Q}) = H^1$;

(iii) $\mathbb{Q}$ *is diagonalizable and has real nonnegative eigenvalues;*

(iv) the linear transformation $\mathbb{Q}(H^1|H^1)$ *is invertible;*

(v) the zero eigenvalue of $\mathbb{Q}$ *has algebraic multiplicity equal to one.*

Proof. We start proving point (ii). Since $\mathrm{Ker}(\mathbb{M}) = H^1_\perp$, one has $\mathbb{M}\mathbb{R}^N = \mathbb{M}(H^1_\perp \oplus H^1) = \mathbb{M}H^1$. Furthermore, from Proposition 1-(iv), $\mathbb{M}H^1 = H^1$. Proposition 1 applied to the Laplacian $\mathbb{L}$ shows that $\mathbb{L}(\mathbb{M}\mathbb{R}^N) = H^1$, which is (ii).

For proving point (i), we notice that $\mathrm{Ker}(\mathbb{M}) = H^1_\perp$ and then $\mathrm{Ker}(\mathbb{L}\mathbb{M}) \supset H^1_\perp$. From (ii) we have that $\dim(\mathrm{Range}(\mathbb{Q})) = N - 1$ and then $\dim(\mathrm{Ker}(\mathbb{Q})) = 1$. Since $\dim(H^1_\perp) = 1$, we have $\mathrm{Ker}(\mathbb{L}\mathbb{M}) = H^1_\perp$.

As regards statement (iii), from [33] we know the product of two complex positive semidefinite matrices is diagonalizable and has nonnegative real eigenvalues. By construction, Laplacians $\mathbb{L}$ and $\mathbb{M}$ are positive semidefinite in the real sense. Moreover, they are symmetric, hence they are positive semidefinite also in the complex sense [20]. Consequently, from [33], we can conclude that point (iii) holds true.

Finally, in order to prove (iv), we exploit Proposition 1. Notably, we have that the linear transformations $\mathbb{L}(H^1|H^1)$ and $\mathbb{M}(H^1|H^1)$ are invertible. Since the composition of invertible maps is invertible, point (iv) follows.

Point (v) follows from points (iii) and (i). Indeed, since $\mathbb{Q}$ is diagonalizable, algebraic and geometric multiplicity of null eigenvalues coincide. From point (i), since $\dim(H^1_\perp) = 1$, we conclude that the null eigenvalue of $\mathbb{Q}$ is unique. □

4.1.1 Analysis of equilibria

In order to evaluate the steady-state behavior of the electrical signals appearing in Figure 4a-4b, we study the equilibria (if any) of system (10). Hence, for given constant inputs $(\mathbf{I}^*_\mathbf{L}, \mathbf{V}^*_\mathbf{ref})$, we compute the solutions $\mathbf{\Delta V}^*$ of equation

$$\mathbb{Q}\mathbf{\Delta V}^* = -\mathbb{L}\mathbf{I}^*_\mathbf{L} - \mathbb{Q}\mathbf{V}^*_\mathbf{ref}. \tag{11}$$

Proposition 3. *For equation* (11)*,*

(i) there is only one solution $\widetilde{\boldsymbol{\Delta \mathbf{V}}}^* \in H^1$*;*

(ii) all solutions $\boldsymbol{\Delta \mathbf{V}}^* \in \mathbb{R}^N$ *can be written as*

$$\boldsymbol{\Delta \mathbf{V}}^* = \widetilde{\boldsymbol{\Delta \mathbf{V}}}^* + \alpha \mathbf{1}_N \quad \alpha \in \mathbb{R}. \tag{12}$$

Proof. Proposition 2-(ii) shows that (11) has solutions only if $-\mathbb{L}\mathbf{I}^*_{\mathbf{L}} - \mathbb{Q}\mathbf{V}^*_{\mathbf{ref}} \in H^1$. From Propositions 1-(iii) and 2-(ii) this is always true. Statement (i) directly follows from Proposition 2-(iv).

For the proof of statement (ii), we split $\boldsymbol{\Delta \mathbf{V}}^* \in \mathbb{R}^N$ as in (1), i.e. $\boldsymbol{\Delta \mathbf{V}}^* = \widehat{\boldsymbol{\Delta \mathbf{V}}}^* + \overline{\boldsymbol{\Delta \mathbf{V}}}^*$. From (11) and Proposition 2-(i), one has that, irrespectively of $\overline{\boldsymbol{\Delta \mathbf{V}}}^* = \alpha \mathbf{1}_N \in H^1_\perp$, $\mathbb{Q}\widehat{\boldsymbol{\Delta \mathbf{V}}}^* = -\mathbb{L}\mathbf{I}^*_{\mathbf{L}} - \mathbb{Q}\mathbf{V}^*_{\mathbf{ref}}$. Moreover, from the above part of the proof, it holds $\widehat{\boldsymbol{\Delta \mathbf{V}}}^* = \widetilde{\boldsymbol{\Delta \mathbf{V}}}^*$. □

Proposition 4. *Consider system* (10) *with constant inputs* $(\mathbf{I}^*_{\mathbf{L}}, \mathbf{V}^*_{\mathbf{ref}})$*. At the equilibrium, proportional current sharing is achieved. Moreover, if* $\mathbf{V}^*_{\mathbf{ref}} = V_{ref}\mathbf{1}_N$ *(i.e. Assumption 1 holds) and* α *in* (12) *is equal to zero, then the equilibrium* $\boldsymbol{\Delta \mathbf{V}}^*$ *ensures also voltage balancing.*

Proof. At the equilibrium, from (6), we have that

$$\mathbf{I}^*_{\mathbf{t}} = \bar{I}_t \mathbf{1}_N, \tag{13}$$

since $\mathrm{Ker}(\mathbb{L}) = H^1_\perp$. Moreover, by substituting (8) in (9), it holds

$$\mathbf{I}^*_{\mathbf{t}} = \mathbf{I}^*_{\mathbf{L}} + \mathbb{M}\mathbf{V}^*. \tag{14}$$

From (14), since $\mathbb{M}\mathbf{V}^* \in H^1$ (see Proposition 1-(iii)), it follows $\langle \mathbf{I}^*_{\mathbf{t}} \rangle = \langle \mathbf{I}^*_{\mathbf{L}} \rangle$. Moreover, from (13), $\bar{I}_t = \langle \mathbf{I}^*_{\mathbf{L}} \rangle$. Consequently, the current sharing condition (3) is verified. Let now $\boldsymbol{\Delta \mathbf{V}}^*$ be an equilibrium for system (10). Replacing (12) in (7) and averaging the obtained vector, we get

$$\langle \mathbf{V}^* \rangle = \underbrace{\langle \widetilde{\boldsymbol{\Delta \mathbf{V}}}^* \rangle}_{=0} + \underbrace{N\alpha}_{=0} + V_{ref},$$

which is the voltage balancing condition (4). □

Through Proposition 4, we have shown the features of the equilibria associated to particular choices of inputs $\mathbf{I_L}$ and $\mathbf{V_{ref}}$. Next, we prove the convergence of $\boldsymbol{\Delta \mathbf{V}}$ in (10) to the equilibrium ensuring both current sharing and voltage balancing (for constant $\mathbf{I_L}^*$ and $\mathbf{V_{ref}}^* = V_{ref}\mathbf{1}_N$), i.e. provide a condition that guarantees α in (12) is equal to zero.

4.1.2 Stability analysis

In order to proceed with the stability analysis of system (10), we consider the dynamics of projections $P_{H^1_\perp}(\boldsymbol{\Delta \mathbf{V}}) = \overline{\boldsymbol{\Delta \mathbf{V}}}$ and $P_{H^1}(\boldsymbol{\Delta \mathbf{V}}) = \widehat{\boldsymbol{\Delta \mathbf{V}}}$.

Proposition 5. *If* $\boldsymbol{\Delta \mathbf{V}}$ *verifies*

$$\Sigma : \begin{cases} \dot{\boldsymbol{\Delta \mathbf{V}}} = -\mathbb{Q}\boldsymbol{\Delta \mathbf{V}} - \mathbb{L}\mathbf{I_L} - \mathbb{Q}\mathbf{V_{ref}} \\ \boldsymbol{\Delta \mathbf{V}}(0) = \boldsymbol{\Delta \mathbf{V}}_0. \end{cases} \tag{15}$$

then $\boldsymbol{\Delta \mathbf{V}} = \overline{\boldsymbol{\Delta \mathbf{V}}} + \widehat{\boldsymbol{\Delta \mathbf{V}}}$*, where* $\overline{\boldsymbol{\Delta \mathbf{V}}} \in H^1_\perp$ *and* $\widehat{\boldsymbol{\Delta \mathbf{V}}} \in H^1$ *fulfill*

$$\overline{\Sigma} : \begin{cases} \dot{\overline{\boldsymbol{\Delta \mathbf{V}}}} = \mathbf{0}_N \\ \overline{\boldsymbol{\Delta \mathbf{V}}}(0) = \langle \boldsymbol{\Delta \mathbf{V_0}} \rangle \mathbf{1}_N \end{cases} \tag{16}$$

and

$$\widehat{\Sigma} : \begin{cases} \dot{\widehat{\boldsymbol{\Delta \mathbf{V}}}} = -\mathbb{Q}\widehat{\boldsymbol{\Delta \mathbf{V}}} - \mathbb{L}\mathbf{I_L} - \mathbb{Q}\mathbf{V_{ref}} \\ \widehat{\boldsymbol{\Delta \mathbf{V}}}(0) = \boldsymbol{\Delta \mathbf{V}}_0 - \overline{\boldsymbol{\Delta \mathbf{V}}}_0. \end{cases} \tag{17}$$

Proof. We write vectors $\mathbf{\Delta V}(0)$, $\mathbf{I_L}$ and $\mathbf{V_{ref}}$ according to the decomposition (1), i.e. using " $\widehat{\ }$ " and " $\overline{\ }$ " for denoting their H^1 and $H^1_\perp$ components, respectively. As described in [22], we analyze the dynamics of $\overline{\mathbf{\Delta V}}$ by averaging both sides of (15). From Proposition 2-(i), we have $\langle -\mathbb{Q}\mathbf{\Delta V}\rangle = \langle -\mathbb{Q}\mathbf{V_{ref}}\rangle = 0$. Since Range$(\mathbb{L}) = H^1$ (see Proposition 1-(iii)), we also have $\langle -\mathbb{L}\mathbf{I_L}\rangle = 0$, hence obtaining $\frac{d}{dt}\langle \mathbf{\Delta V}\rangle = 0$. Recalling that $\overline{\mathbf{\Delta V_0}} = \langle \mathbf{\Delta V_0}\rangle \mathbf{1}_N$, we obtain (16).

Next, we analyze $\widehat{\mathbf{\Delta V}} = \mathbf{\Delta V} - \overline{\mathbf{\Delta V}}$. We have

$$\dot{\widehat{\mathbf{\Delta V}}} = \dot{\mathbf{\Delta V}} - \underbrace{\dot{\overline{\mathbf{\Delta V}}}}_{=\mathbf{0}_N} = -\mathbb{Q}\mathbf{\Delta V} - \mathbb{L}\mathbf{I_L} - \mathbb{Q}\mathbf{V_{ref}}$$

and $\widehat{\mathbf{\Delta V}}(0) = \mathbf{\Delta V}_0 - \overline{\mathbf{\Delta V}}_0$. From Proposition 2-(i), $\mathbb{Q}\mathbf{\Delta V} = \mathbb{Q}\widehat{\mathbf{\Delta V}}$ and then we have (17). □

Remark 3. *The splitting of Σ into systems $\overline{\Sigma}$ and $\widehat{\Sigma}$ implies that the subspace H^1 is invariant for Σ and $(\mathbf{I_L}, \mathbf{V_{ref}}) \in \mathbb{R}^N \times \mathbb{R}^N$. Recalling that $\mathbb{L}\mathbf{I_L} = \mathbf{0}_N$ for $\mathbf{I_L} \in H^1_\perp$ and $\mathbb{Q}\mathbf{V_{ref}} = \mathbf{0}_N$ for $\mathbf{V_{ref}} \in H^1_\perp$, system $\overline{\Sigma}$ shows that the subspace $H^1_\perp$ is invariant for Σ and $(\mathbf{I_L}, \mathbf{V_{ref}}) \in H^1_\perp \times H^1_\perp$. Consequently, in order to...*

According to system $\overline{\Sigma}$, the value of $P_{H^1_\perp}(\mathbf{\Delta V}) = \overline{\mathbf{\Delta V}}$ remains constant over time and equal to $\overline{\mathbf{\Delta V_0}}$. Hence, in order to characterize the stability of equilibria (12), it is sufficient to study the dynamics (17). In an equivalent way, one can consider system (15) and the following definition of stability on a subspace.

Definition 3. *Let $\mathcal{V}$ be a subspace of $\mathbb{R}^n$. The origin of $\dot{x} = \mathcal{A}x$, $x(t) \in \mathbb{R}^n$ is Globally Exponentially Stable (GES) on $\mathcal{V}$ if $\exists \kappa, \eta > 0$: $\|P_{\mathcal{V}}x(t)\| \leq \kappa e^{-\eta t}\|P_{\mathcal{V}}x(0)\|$. The parameter η is termed rate of convergence.*

Note that Σ is a linear system and, for stability analysis, we can neglect inputs, hence obtaining

$$\begin{cases} \dot{\mathbf{\Delta V}} = -\mathbb{Q}\mathbf{\Delta V} \\ \mathbf{\Delta V}(0) = \mathbf{\Delta V}_0. \end{cases} \tag{18}$$

Theorem 1. *The origin of* (18) *is GES on H^1. Moreover, the rate of convergence is the smallest strictly positive eigenvalue of $\mathbb{Q}$.*

Proof. The proof of Theorem 1 is reported in Appendix A. □

From the above results, we can conclude that, given an initial condition $\mathbf{\Delta V_0}$ for system (15) and applying constant inputs $\mathbf{I_L}^*$ and $\mathbf{V_{ref}} = V_{ref}\mathbf{1}_N$, the state $\mathbf{\Delta V}$ will converge to the equilibrium (12) with $\alpha = \langle \mathbf{\Delta V_0}\rangle$.

Corollary 1. *The conditions that ensure asymptotic current sharing and voltage balancing for system* (15) *are Assumption 1 and*

$$\langle \mathbf{\Delta V_0}\rangle = 0. \tag{19}$$

Proof. The proof directly follows from Proposition 4. □

4.2 First-order approximation of PnP-controlled DGUs

In this Section, we adopt a less restrictive approximation of DGUs equipped with primary PnP regulators, and provide conditions guaranteeing current sharing and voltage balancing in the asymptotic régime. Figure 4a-4c shows the overall closed-loop scheme of an mG equipped with (i) consensus current loops and (ii) local control loops (each given by a DGU and the corresponding PnP controller) modeled as first-order transfer functions. Differently from the case analyzed in Section 4.1, each local dynamics is now described by means of two states which are the state of the consensus current loop (ΔV_i) and the state of the controlled DGU (V_i in Figure 4c). We highlight that relations (6) and (7) still hold, while the additional state equation is

$$\dot{\mathbf{V}} = \Omega\mathbf{V}^\circ - \Omega\mathbf{V}, \tag{20}$$

where vectors $\mathbf{V}^\circ = [V_1^\circ, V_2^\circ, \dots, V_N^\circ]^T$ and $\mathbf{V}$ belong to $\mathbb{R}^N$, and the diagonal matrix $\Omega = \omega_c I \in \mathbb{R}^{N\times N}$, $\omega_c > 0$, collects on its diagonal the approximate bandwidth of each controlled DGU. In view of Remark 2, assuming equal approximate bandwidths for all the controlled DGUs is a mild constraint.

Similarly to the simplified case in Section 4.1, in order to find the dynamics of the closed-loop scheme, we write relations among mG variables. From Figure 4a, we notice that (6) holds, and

$$\mathbf{V}^\circ = \boldsymbol{\Delta}\mathbf{V} + \mathbf{V_{ref}}. \tag{21}$$

Always from Figure 4a, we have that, for line and output currents, equations (8) and (9) are still valid. By merging relations (6), (21), (20), (8) and (9), we can write the dynamics of the overall mG as

$$\begin{cases} \dot{\boldsymbol{\Delta}\mathbf{V}} = -\mathbb{Q}\mathbf{V} - \mathbb{L}\mathbf{I_L} & \text{(22a)} \\ \dot{\mathbf{V}} = \Omega\boldsymbol{\Delta}\mathbf{V} - \Omega\mathbf{V} + \Omega\mathbf{V_{ref}}, & \text{(22b)} \end{cases}$$

or, equivalently, in compact form,

$$\begin{bmatrix} \dot{\boldsymbol{\Delta}\mathbf{V}} \\ \dot{\mathbf{V}} \end{bmatrix} = \underbrace{\begin{bmatrix} \mathbf{0}_N & -\mathbb{Q} \\ \Omega & -\Omega \end{bmatrix}}_{\mathcal{Q}} \begin{bmatrix} \boldsymbol{\Delta}\mathbf{V} \\ \mathbf{V} \end{bmatrix} + \begin{bmatrix} \mathbf{0}_N & -\mathbb{L} \\ \Omega & -\Omega \end{bmatrix} \begin{bmatrix} \mathbf{V_{ref}} \\ \mathbf{I_L} \end{bmatrix}, \tag{23}$$

with $\mathcal{Q} \in \mathbb{R}^{2N\times 2N}$ and $[\boldsymbol{\Delta}\mathbf{V}^T \mathbf{V}^T]^T \in \mathbb{R}^N \times \mathbb{R}^N$.

4.2.1 Analysis of equilibria

Similarly to Section 4.1.1, we study the equilibria of system (22). For this purpose, given the constant inputs $(\mathbf{I_L}^*, \mathbf{V_{ref}}^*)$, we compute the solutions $[\boldsymbol{\Delta}\mathbf{V}^{*T}, \mathbf{V}^{*T}]^T$ to the system

$$\begin{cases} \mathbb{Q}\mathbf{V}^* = -\mathbb{L}\mathbf{I_L^*} & \text{(24a)} \\ \mathbf{0}_N = \Omega\boldsymbol{\Delta}\mathbf{V}^* - \Omega\mathbf{V}^* + \Omega\mathbf{V_{ref}^*}. & \text{(24b)} \end{cases}$$

Since matrix Ω is invertible, equation (24b) becomes

$$\mathbf{V}^* = \boldsymbol{\Delta}\mathbf{V}^* + \mathbf{V_{ref}^*}. \tag{25}$$

By substituting (25) in (24a), we get

$$\mathbb{Q}\boldsymbol{\Delta}\mathbf{V}^* = -\mathbb{L}\mathbf{I_L^*} - \mathbb{Q}\mathbf{V_{ref}^*}.$$

that is exactly (11). We can then exploit Proposition 3 for concluding that there are infinitely many solutions $\boldsymbol{\Delta}\mathbf{V}^* \in \mathbb{R}^N$ in the form (12). Replacing (12) in (25), we can write equilibria of system (22) as

$$\begin{bmatrix} \boldsymbol{\Delta}\mathbf{V}^* \\ \mathbf{V}^* \end{bmatrix} = \begin{bmatrix} \widehat{\boldsymbol{\Delta}\mathbf{V}}^* + \alpha\mathbf{1}_N \\ \widehat{\boldsymbol{\Delta}\mathbf{V}}^* + \alpha\mathbf{1}_N + \mathbf{V_{ref}^*} \end{bmatrix}. \tag{26}$$

Proposition 6. *Consider system* (22) *with constant inputs* $\mathbf{I_L^*}$ *and* $\mathbf{V_{ref}^*}$. *At the equilibrium, current sharing is achieved. Moreover, if* $\mathbf{V_{ref}^*} = V_{ref}^* \mathbf{1}_N$ *(i.e. Assumption 1 holds) and* α *in* (26) *is equal to zero, then the equilibrium* $[\boldsymbol{\Delta}\mathbf{V}^{*T}, \mathbf{V}^{*T}]^T$ *guarantees also voltage balancing.*

Proof. Since equation (6) holds, one has that, at the equilibrium, relation (13) is verified. Then, the proof is the same as the one of Proposition 4. □

4.2.2 Stability analysis

Proposition 7. *If* $[\mathbf{\Delta V}^T \mathbf{V}^T]^T$ *verifies* (22)*, then*

$$\underbrace{\begin{bmatrix} \mathbf{\Delta V} \\ \mathbf{V} \end{bmatrix}}_{\mathbf{v}} = \underbrace{\begin{bmatrix} \overline{\mathbf{\Delta V}} \\ \overline{\mathbf{V}} \end{bmatrix}}_{\bar{\mathbf{v}}} + \underbrace{\begin{bmatrix} \widehat{\mathbf{\Delta V}} \\ \widehat{\mathbf{V}} \end{bmatrix}}_{\hat{\mathbf{v}}},$$

where $\bar{\mathbf{v}} \in H^1_\perp \times H^1_\perp$ *and* $\hat{\mathbf{v}} \in H^1 \times H^1$ *fulfill*

$$\widetilde{\Sigma}^1_\perp : \begin{cases} \dot{\overline{\mathbf{\Delta V}}} = \mathbf{0}_N & (27a) \\ \dot{\overline{\mathbf{V}}} = \Omega \overline{\mathbf{\Delta V}} - \Omega \overline{\mathbf{V}} + \Omega \overline{\mathbf{V_{ref}}} & (27b) \end{cases}$$

and

$$\widetilde{\Sigma}^1 : \begin{cases} \dot{\widehat{\mathbf{\Delta V}}} = -\mathbb{Q} \widehat{\mathbf{V}} - \mathbb{L} \mathbf{I_L} & (28a) \\ \dot{\widehat{\mathbf{V}}} = \Omega \widehat{\mathbf{\Delta V}} - \Omega \widehat{\mathbf{V}} + \Omega \widehat{\mathbf{V_{ref}}}, & (28b) \end{cases}$$

respectively.

Proof. The dynamics of $\overline{\mathbf{\Delta V}}$ and $\widehat{\mathbf{\Delta V}}$ can be derived proceeding as in the proof of Proposition 5. In a similar way, by averaging both sides of (22b), one derives the (independent) dynamics of $\overline{\mathbf{V}}$ and $\widehat{\mathbf{V}}$. □

The above decomposition allows us to evaluate the evolution of state $\mathbf{v}$ on $\mathbb{R}^{N \times N}$ by separately analyzing dynamics (27) and (28), i.e. studying the behavior of projections $\bar{\mathbf{v}} = P_{\mathcal{V}}(\mathbf{v})$ and $\hat{\mathbf{v}} = P_{\mathcal{W}}(\mathbf{v})$, with $\mathcal{V} = H^1_\perp \times H^1_\perp$ and $\mathcal{W} = H^1 \times H^1$.

First we focus on $\tilde{\Sigma}^1_\perp$. Without loss of generality, for stability analysis we can neglect the input vector $\overline{\mathbf{V_{ref}}}$ in (27b), thus having:

$$\begin{cases} \dot{\overline{\mathbf{\Delta V}}} = \mathbf{0}_N & (29a) \\ \dot{\overline{\mathbf{V}}} = \Omega \overline{\mathbf{\Delta V}} - \Omega \overline{\mathbf{V}}. & (29b) \end{cases}$$

By construction, (29b) collects the decoupled equations

$$\dot{\overline{V}}_i = \omega_c \overline{\Delta V_i} - \omega_c \overline{V}_i \quad \forall i = 1, \dots, N, \tag{30}$$

where, according to (27a), each term $\overline{\Delta V_i}$ in can be treated as an exogenous input (thus not affecting stability properties). It follows that dynamics (30) is asymptotically stable, since $\omega_c > 0$. In summary, system (27) tells us that the average $\overline{\mathbf{\Delta V}}$ will remain constant in time (and equal to $\langle \mathbf{\Delta V_0} \rangle$), while $\overline{\mathbf{V}}$ will converge to the origin. For studying stability properties of system $\widetilde{\Sigma}^1$, we consider (22) without inputs, i.e.

$$\begin{cases} \dot{\mathbf{\Delta V}} = -\mathbb{Q} \mathbf{V} \\ \dot{\mathbf{V}} = \Omega \mathbf{\Delta V} - \Omega \mathbf{V} \end{cases} \tag{31}$$

and analyze stability on $H^1 \times H^1$. We have the following result.

Theorem 2. *The origin of* (31) *is GES on* $H^1 \times H^1$*. Furthermore, matrix* $\mathcal{Q}$ *has a simple zero eigenvalue and the rate of convergence is the maximum among real parts of all other eigenvalues.*

Proof. The proof is given in Appendix B. □

By means of Theorem 2, we have that, given an initial condition $[\mathbf{\Delta V_0}^T \mathbf{V_0}^T]^T$ for system (22), the state $[\mathbf{\Delta V}^T \mathbf{V}^T]^T$ will converge to the equilibrium in (26). with $\alpha = \langle \mathbf{\Delta V_0} \rangle$

Corollary 2. *The conditions that ensure asymptotic current sharing and voltage balancing for system* (22) *are Assumption 1 and* (19)*.*

Proof. The proof follows from Proposition 6. □

4.3 PnP design of secondary control

We now describe the procedure for designing secondary controllers in a PnP fashion.

When a DGU (say DGU i) sends a plug-in request at a time $\bar{t}$, a set $\mathcal{N}_i^c$ of "communication neighbors" with $a_{ij} = 1, \forall j \in \mathcal{N}_i^c$, is also chosen in order to design local consensus filters (6). Theorems 1 and 2 ensure that the mG is GES over suitable subspaces, independently of $\mathcal{N}_i^c$. Let Assumption 1 hold for all the interconnected DGUs in the mG before $\bar{t}$ and let us denote the common reference voltage by V_{ref}. If DGU i sets $V_{ref,i} = V_{ref}$, then, according to Propositions 4 and 6, current sharing and voltage balancing are guaranteed in the asymptotic régime. Moreover, by choosing $\Delta V_i(\bar{t}) = 0$, we have $\langle \begin{bmatrix} \mathbf{\Delta V}'(\bar{t}) \\ \Delta V_i(\bar{t}) \end{bmatrix} \rangle = 0$, where $\mathbf{\Delta V}'(\bar{t})$ is the vector $\mathbf{\Delta V}$ prior the plugging in of DGU i. Therefore, by means of Corollaries 1 and 2, voltage balancing is guaranteed. Similarly, when a DGU (say DGU j) is unplugged at time $\bar{t}$, provided that the new graphs $\mathcal{G}_c$ and $\mathcal{G}_{el}$ fulfill Assumption 3, the key condition that must be guaranteed is that the vector $\mathbf{\Delta V_{-j}}$ (i.e. $\mathbf{\Delta V}$ without element j) verifies $\langle \mathbf{\Delta V_{-j}}(\bar{t}) \rangle = 0$. If $\langle \mathbf{\Delta V}(\bar{t}^-) \rangle = 0$, this can be achieved by re-setting

$$\Delta V_i(\bar{t}) = \Delta V_i(\bar{t}^-) + \frac{\Delta V_j(\bar{t}^-)}{|\mathcal{N}_j^c|}$$

for all $i \in \mathcal{N}_j^c$, and keeping $\Delta V_i(\bar{t}) = \Delta V_i(\bar{t}^-)$ for all $i \notin \mathcal{N}_j^c \cup \{j\}$. Indeed, this yields

$$\begin{aligned}
\langle \mathbf{\Delta V_{-j}}(\bar{t}) \rangle &= \frac{1}{N-1} \sum_{i \in \mathcal{N}_j^c} \Delta V_i(\bar{t}) + \frac{1}{N-1} \sum_{i \notin \mathcal{N}_j^c \cup \{j\}} \Delta V_i(\bar{t}) \\
&= \frac{1}{N-1} \left(\sum_{i \in \mathcal{N}_j^c} \Delta V_i(\bar{t}^-) + \frac{1}{|\mathcal{N}_j^c|} \sum_{i \in \mathcal{N}_j^c} \Delta V_j(\bar{t}^-) + \sum_{i \notin \mathcal{N}_j^c \cup \{j\}} \Delta V_i(\bar{t}^-) \right) = \\
&= \frac{1}{N-1} \left(N \langle \mathbf{\Delta V}(\bar{t}^-) \rangle \right) = 0.
\end{aligned}$$

5 Simulation results

In this Section, we assess the capability of the proposed control scheme to guarantee current sharing and voltage balancing while preserving overall voltage stability when plug-in of DGUs or load changes occur. Simulations have been performed in Simulink/PLECS.

We consider an mG composed of 5 DGUs, arranged as in Figure 5. Notice that some DGUs have more than one neighbor, hence load disturbances influencing their dynamics will be greater. Moreover, the presence of a loop in the electrical network further complicates voltage regulation. We highlight that the considered mG is composed of nonidentical DGUs and heterogeneous power lines. All the electrical and control parameters are collected in Tables 2 and 3 in Appendix C, respectively. Furthermore, Assumption 1 holds, with $V_{ref} = 48$ V.

We show two simulations, assuming different communication graphs. Both scenarios are divided into 4 stages, as shown in Figure 5.

5.1 Scenario 1

In the following, we describe in details Figure 7, which illustrates the evolution of the main electrical quantities (i.e. DGU output currents, PCC voltages and averaged PCC voltage, respectively) when $\mathcal{G}_c$ and $\mathcal{G}_{el}$ have the same topology. At time $t_0 = 0$, all the DGUs are assumed to be isolated and only the primary PnP voltage regulators are active. Therefore, as shown in stage 1, (i) each DGU supplies its local load while keeping the corresponding PCC voltage at 48 V, and (ii) the DGU output currents are different. Notice that DGUs 1-4 are equipped with controllers $\mathcal{C}_{[i]}$ designed by taking into account couplings among them. This is possible because, as shown [10], local PnP controllers stabilize the mG also in absence of couplings. Because of this, when stage 2 starts (at time $t_1 = 5$ s) and subsystems 1-4 are connected together, no update of controllers is needed.

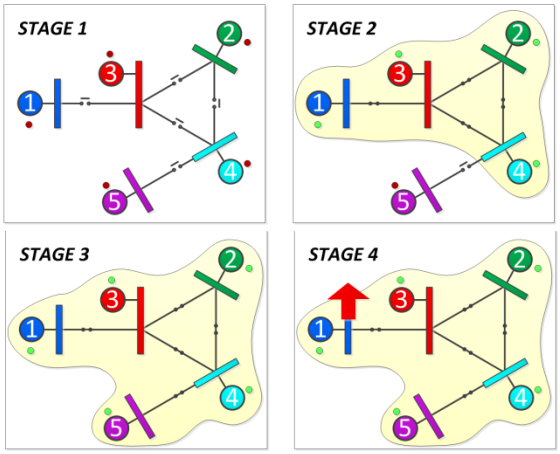

Figure 5: Simulation stages: numbered nodes represent DGUs and black lines denote power lines. The small circle next to each DGU is green if the secondary control layer is active for the corresponding unit, red otherwise. Open switches in stages 1 and 2 denote DGUs that are disconnected. The arrow in stage 4 represents a step up in the load current of DGU 1.

At time t_1, we also activate the secondary control layer for DGUs 1-4, thus ensuring asymptotic current sharing among them according to their capacities (see the plot of I_t, stage 2). This is achieved by adjusting the voltages at PCC (as shown in the plot of V_{PCC}, stage 2). Furthermore, by setting $\Delta V_i(t_1) = 0$, $i = 1, \ldots, 4$ as described in Section 4.3, condition (19) of Corollaries 1 and 2 are fulfilled and asymptotic voltage balancing, when DGUs 1-4 are interconnected, is guaranteed (see V_{av} during stage 2).

For evaluating the PnP capabilities of our control scheme, at $t_2 = 25$ s, stage 3 starts with DGU 5 sending a plug-in request to DGU 4. Previous controllers $\mathcal{C}_{[4]}$ and $\mathcal{C}_{[5]}$ still fulfill the plug-in conditions in [10]: they are therefore maintained and the plug-in of DGU 5 is performed. At the same time, the secondary controller of DGU 5 is activated, and then the DGU contributes to current sharing. This can be noticed in Figure 7, stage 3, as all PCC voltages change in order to let the output currents of DGUs 1-5 converge to a common value. Furthermore, by setting $\Delta V_5(t_2) = 0$ (as described in Section 4.3), we can maintain the average PCCs voltage at 48 V (see V_{av}, stage 3).

Finally, at $t_3 = 50$ s (stage 4), we halve the load of DGU 1, thus increasing the corresponding load current I_{L1} and causing a peak in the corresponding output current. However, after few seconds, all the DGUs share again the total load current, while the averaged PCCs voltage converges to the reference value.

5.2 Scenario 2

In this second scenario, we assume all-to-all communication among DGUs. The simulation time events are summarized in Table 1.

Time [s]	Event
$t_0 = 0$	Start simulation
$t_1 = 5$	stage 1 $\rightarrow$ stage 2
$t_2 = 16$	stage 2 $\rightarrow$ stage 3
$t_3 = 30$	stage 3 $\rightarrow$ stage 4
$t_4 = 40$	End simulation

Table 1: Scenario 2 - Simulation time events.

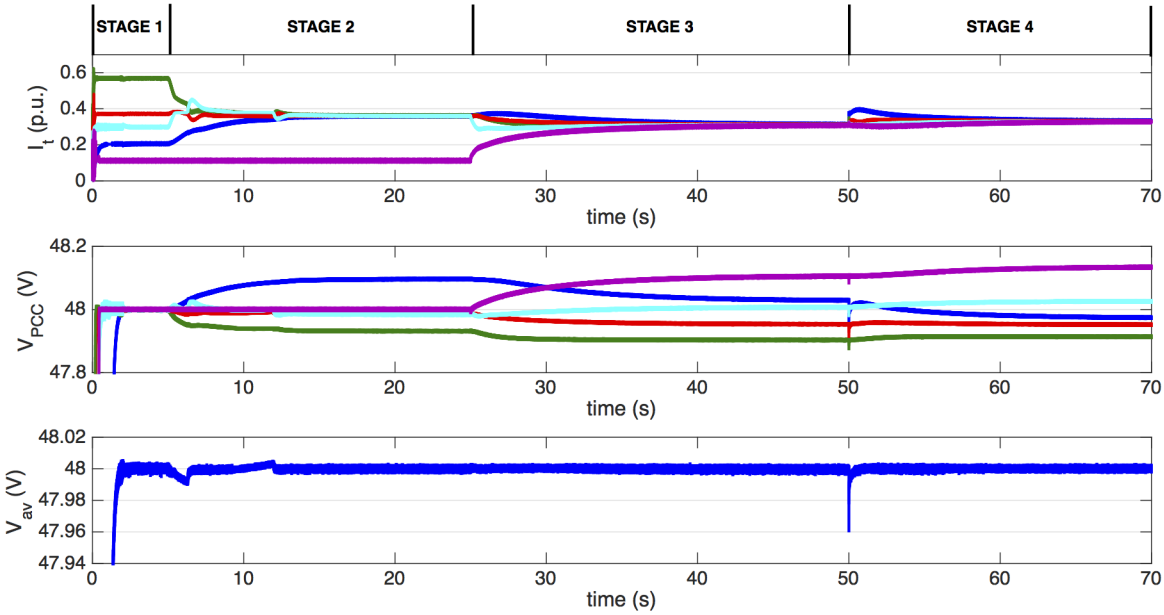

Figure 6: Scenario 1 - Evolution of the output currents, voltages at PCCs and averaged PCCs voltage. Colored lines in the plots of I_t and V_{PCC} are used to denote the DGUs quantities according to Figure 5. Simulation stages are the same as in Figure 5.

Figure 7 shows the evolution of the main electrical quantities. We notice that the proposed control schemes is capable to guarantee all the desired properties (i.e. overall mG stability, robustness to load changes, current sharing and voltage balancing). As expected, a full-connected communication graph ensures faster convergence of the output currents when the secondary control layer is activated (see stages 2, 3 and 4 in Figure 7).

6 Conclusions

In this paper, a secondary consensus-based control layer for guaranteeing current sharing and voltage balancing in DC mGs has been presented. Besides overall mG stability, current sharing and voltage balancing have been rigorously proved in the asymptotic régime. Moreover, we presented a method for designing secondary controllers in a PnP fashion when DGUs are added. As regards future developments, communication delays [34, 35], may be included in the mathematical analysis, as well as more complex consensus controllers (e.g. proportional-integral regulators) for enhancing the convergence speed.

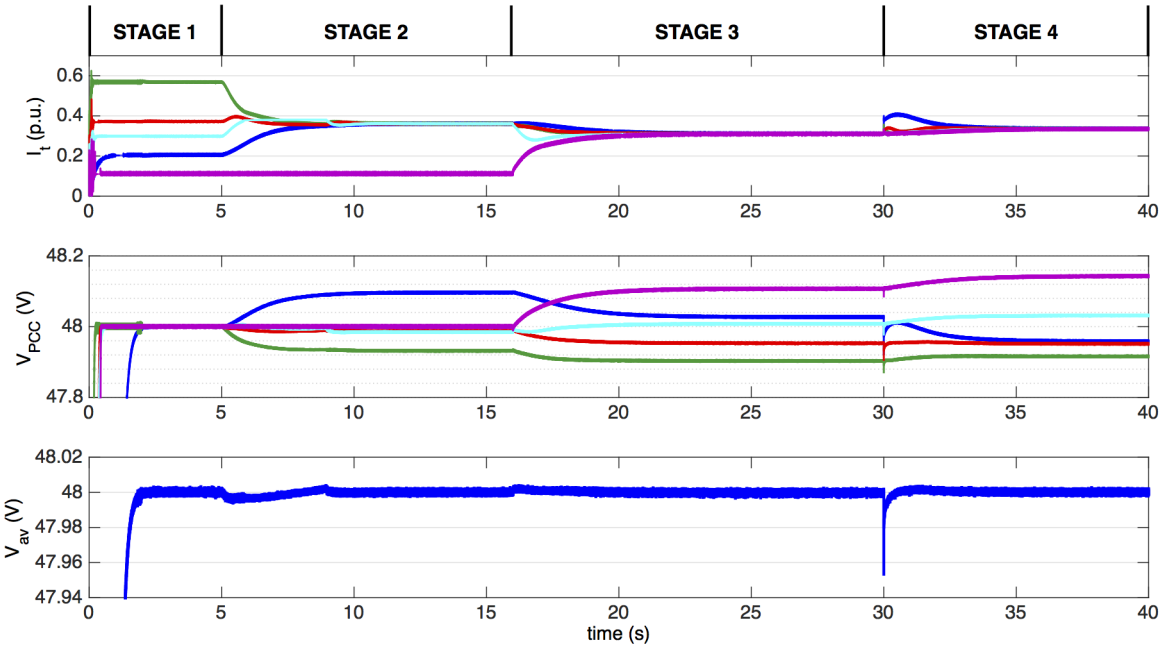

Figure 7: Scenario 2 - Evolution of the output currents, voltages at PCCs and averaged PCCs voltage. Colored lines in the plots of I_t and V_{PCC} are used to denote the DGUs quantities according to Figure 5. Simulation stages are the same as in Figure 5.

A Proof of Theorem 1

We introduce a preliminary Lemma, mainly taken from [23].

Lemma 1. *For $\mathcal{A} \in \mathbb{R}^{n\times n}$, let $\mathcal{V}$ and $\mathcal{W}$ be $\mathcal{A}$-invariant subspaces of $\mathbb{R}^n$ such that $dim(\mathcal{V}) = k$, $dim(\mathcal{W}) = n-k$ and $\mathbb{R}^n = \mathcal{V} \oplus \mathcal{W}$. Then:*

I) there is a matrix $T \in \mathbb{R}^{n\times n}$ such that $A = T^{-1}\mathcal{A}T$ has the block-diagonal structure

$$A = \begin{bmatrix} \overbrace{A_{11}}^{k} & \overbrace{\mathbf{0}}^{n-k} \\ \mathbf{0} & A_{22} \end{bmatrix} \begin{matrix} \} k \\ \} n-k \end{matrix} \tag{32}$$

In particular, if $\{b_1, \dots, b_k\}$ and $\{b_{k+1}, \dots, b_n\}$ are basis for $\mathcal{V}$ and $\mathcal{W}$, respectively, the transformation matrix T has the block structure

$$T = [b_1|\cdots|b_k|b_{k+1}|\cdots|b_n]. \tag{33}$$

Therefore, if $x \in \mathcal{V}$, then $T^{-1}x = \left[\frac{\tilde{x}_1}{0}\right]$ with $\tilde{x}_1 \in \mathbb{R}^k$. Similarly, if $x \in \mathcal{W}$, then $T^{-1}x = \left[\frac{0}{\tilde{x}_2}\right]$ with $\tilde{x}_2 \in \mathbb{R}^{n-k}$.

II) The origin of $\dot{x} = \mathcal{A}x$ is GES on $\mathcal{V}$ if and only if the origin of $\dot{\tilde{x}}_1 = A_{11}\tilde{x}_1$ is GES. Moreover, parameters $\kappa, \eta > 0$ verifying $\|\tilde{x}_1(t)\| \leq \kappa e^{-\eta t}\|\tilde{x}_1(0)\|$, also guarantee $\|P_{\mathcal{V}}x(t)\| \leq \kappa e^{-\eta t}\|P_{\mathcal{V}}x(0)\|$.

Proof. For the proof of Point I, we defer the reader to the proof of Theorem 19 in [23].

The proof of Point II directly follows from the block-diagonal structure of matrix A in (32). Indeed,

$$\dot{x} = \mathcal{A}x \Leftrightarrow \dot{\tilde{x}} = A\left[\frac{\tilde{x}_1}{\tilde{x}_2}\right] \Leftrightarrow \quad \begin{cases} \dot{\tilde{x}}_1 = A_{11}\tilde{x}_1 \\ \dot{\tilde{x}}_2 = A_{22}\tilde{x}_2, \end{cases}$$

i.e. A_{11} is the matrix representation of the map $\mathcal{A}(\mathcal{V}|\mathcal{V})$. In other words, studying the stability of $\mathcal{A}$ on $\mathcal{V}$ is equivalent to study the stability of A_{11}.

Moreover, by construction, $P_{\mathcal{V}}(x) = T\left[\frac{\tilde{x}_1}{0}\right]$. Then

$$\|P_{\mathcal{V}}(x(t))\| \leq \|T\|\|\tilde{x}_1(t)\| \leq \|T\|\kappa e^{-\eta t}\|\tilde{x}_1(0)\|. \tag{34}$$

Since $\|\tilde{x}_1(0)\| \leq \|T^{-1}\|\|P_{\mathcal{V}}(x(0))\|$, inequality (34) becomes

$$\|P_{\mathcal{V}}(x)\| \leq \|T\|\kappa e^{-\eta t}\|\tilde{x}_1(0)\| \leq \kappa e^{-\eta t}\|P_{\mathcal{V}}(x(0))\|.$$

□

Proof of Theorem 1. Points (i) and (ii) of Proposition 2 show that subspaces H^1 and $H^1_\perp$ are $\mathbb{Q}$-invariant. Moreover, $\mathbb{R}^N = H^1 \oplus H^1_\perp$. It follows that Lemma 1 can be applied with $\mathcal{V} = H^1$ and $\mathcal{W} = H^1_\perp$. In particular, by means of point (I), we know that there exists a transformation matrix $T \in \mathbb{R}^{N\times N}$ such that the linear map $\mathbb{Q}$ can be represented as in (32). Denoting with $B^1 = \{b_1, \dots, b_{N-1}\}$ and $B^1_\perp = \mathbf{1}_N$ the basis for H^1 and $H^1_\perp$, respectively, from (33), we have

$$T = [b_1|\cdots|b_{N-1}|\mathbf{1}_N].$$

Matrix $Q = T^{-1}\mathbb{Q}T$ is given by

$$Q = \begin{bmatrix} Q_{11} & \mathbf{0} \\ \mathbf{0} & q_{22} \end{bmatrix} \tag{35}$$

where $Q_{11} \in \mathbb{R}^{(N-1)\times(N-1)}$. Moreover, scalar $q_{22} = 0$ since, by construction, it represents the map $\mathbb{Q}(H^1_\perp | H^1_\perp)$. We notice that the representations of $\widehat{\mathbf{\Delta V}}$ and $\overline{\mathbf{\Delta V}}$ with respect to the basis $\mathcal{B}$ are $\tilde{v}_1 = T^{-1}\widehat{\mathbf{\Delta V}} = [\xi_1, \dots, \xi_{N-1}, 0]^T$ and $\tilde{v}_\perp = T^{-1}\overline{\mathbf{\Delta V}} = [0, \dots, 0, \xi_N]^T$, respectively. Now we prove that the origin of

$$\dot{\tilde{v}}_1 = -Q_{11}\tilde{v}_1 \tag{36}$$

is GES. Since Q and $\mathbb{Q}$ are similar matrices, they have the same eigenvalues. Therefore, from Proposition 2-(iii), all eigenvalues of Q_{11} are strictly positive. This shows that (36) is GES and, as shown in [23], the convergence rate is $-\lambda$, where λ is the minimal eigenvalue of Q_{11}. The remainder of the proof follows directly from point II of Lemma 1. □

B Proof of Theorem 2

We first present two Propositions which provide preliminary results that will be used to prove Theorem 2.

Proposition 8. *Subspaces $H^1 \times H^1$ and $H^1_\perp \times H^1_\perp$ are $\mathcal{Q}$-invariant.*

Proof. We first show that, for any vector $\hat{\mathbf{v}} = [\hat{\mathbf{v}}_\mathbf{1}^T \hat{\mathbf{v}}_\mathbf{2}^T]^T$, it holds $\mathcal{Q}\hat{\mathbf{v}} \in H^1 \times H^1$. Indeed,

$$\mathcal{Q}\hat{\mathbf{v}} = \begin{bmatrix} \mathbf{0}_N & -\mathbb{Q} \\ \Omega & -\Omega \end{bmatrix} \begin{bmatrix} \hat{\mathbf{v}}_\mathbf{1} \\ \hat{\mathbf{v}}_\mathbf{2} \end{bmatrix} = \begin{bmatrix} \mathbb{Q}\hat{\mathbf{v}}_\mathbf{1} \\ \Omega(\hat{\mathbf{v}}_\mathbf{1} - \hat{\mathbf{v}}_\mathbf{2}) \end{bmatrix},$$

and, from Proposition 2-(iv), the rightmost vector belongs to $H^1 \times H^1$.

Similarly, for any vector $\bar{\mathbf{v}} = [\bar{\mathbf{v}}_\mathbf{1}^T \bar{\mathbf{v}}_\mathbf{2}^T]^T \in H^1_\perp \times H^1_\perp$, we have that

$$\mathcal{Q}\hat{\mathbf{v}} = \begin{bmatrix} \mathbf{0}_N & -\mathbb{Q} \\ \Omega & -\Omega \end{bmatrix} \begin{bmatrix} \bar{\mathbf{v}}_\mathbf{1} \\ \bar{\mathbf{v}}_\mathbf{2} \end{bmatrix} = \begin{bmatrix} \mathbf{0}_N \\ \Omega(\bar{\mathbf{v}}_\mathbf{1} - \bar{\mathbf{v}}_\mathbf{2}) \end{bmatrix}$$

and then $\mathcal{Q}\bar{\mathbf{v}} \in H^1_\perp \times H^1_\perp$. □

Proposition 9. *Matrix $\mathcal{Q}$ has two eigenvalues equal to zero and $-\omega_c$, respectively. All other eigenvalues have strictly negative real part.*

Proof. By definition, vector $[\mathbf{\Delta V}^T \mathbf{V}^T]^T \neq \mathbf{0}_{2N}$ is an eigenvector of $\mathcal{Q}$, if there exists λ_i such that

$$\begin{bmatrix} \mathbf{0} & -\mathbb{Q} \\ \Omega & -\Omega \end{bmatrix} \begin{bmatrix} \mathbf{\Delta V} \\ \mathbf{V} \end{bmatrix} = \lambda_i \begin{bmatrix} \mathbf{\Delta V} \\ \mathbf{V} \end{bmatrix}. \tag{37}$$

From (37), one gets:

$$-\mathbb{Q}\mathbf{V} = \lambda_i \mathbf{\Delta V} \tag{38a}$$

$$\omega_c(\widehat{\mathbf{\Delta V}} - \mathbf{V}) = \lambda_i \mathbf{V}. \tag{38b}$$

By isolating $\mathbf{\Delta V}$ in (38b) and substituting it in (38a), we obtain

$$-\mathbb{Q}\mathbf{V} = \underbrace{\frac{\lambda_i(\lambda_i + \omega_c)}{\omega_c}}_{\widehat{\lambda}_i} \mathbf{V}. \tag{39}$$

where $\hat{\lambda}_i$ are, by construction, eigenvalues of $-\mathbb{Q}$. From points (iii) and (v) of Proposition 2, we have

$$\hat{\lambda}_N = 0 \tag{40a}$$

$$\hat{\lambda}_i = -\gamma_i, \;\; \gamma_i > 0 \qquad i = 1, \dots, N-1. \tag{40b}$$

From (40a) and (39), one has

$$\lambda_i(\lambda_i + \omega_c) = 0$$

and hence $\mathcal{Q}$ has a single eigenvalue equal to zero and an eigenvalue equal to $-\omega_c$. By substituting in (40b) the expression of $\hat{\lambda}_i$ in (39), one gets:

$$\frac{\lambda_i^2}{\omega_c} + \lambda_i + \gamma_i = 0 \qquad i = 1, \dots, N-1. \tag{41}$$

Since all the coefficients of the polynomial in (41) are strictly positive, we can conclude that matrix $\mathcal{Q}$ has $2(N-1)$ eigenvalues with $\mathrm{Re}(\lambda_i) < 0$. □

Proof of Theorem 2. Similarly to the proof of Theorem 1, we can exploit Lemma 1 with $\mathcal{V} = H^1 \times H^1$ and $\mathcal{W} = H^1_\perp \times H^1_\perp$. In fact, we know that (i) subspaces $H^1 \times H^1$ and $H^1_\perp \times H^1_\perp$ are $\mathcal{Q}$-invariant (see Proposition 8) and (ii) $\mathbb{R}^N \times \mathbb{R}^N = \mathcal{V} \oplus \mathcal{W}$. Hence, there exists a transformation matrix $T \in \mathbb{R}^{2N \times 2N}$ such that the linear map $\mathcal{Q}$ has an equivalent block-diagonal representation of the form (32), i.e.

$$T^{-1}\mathcal{Q}T = Q = \begin{bmatrix} \overbrace{Q_{11}}^{2(N-1)} & \overbrace{\mathbf{0}}^{2} \\ \mathbf{0} & Q_{22} \end{bmatrix} \begin{matrix} \} 2(N-1) \\ \} 2 \end{matrix} \tag{42}$$

By construction, matrices Q_{11} and Q_{22} in (42) represent the maps $\mathcal{Q}(\mathcal{V}|\mathcal{V})$ and $\mathcal{Q}(\mathcal{W}|\mathcal{W})$, respectively. In particular, in the light on the consideration made for system (27), we have that the eigenvalues of Q_{22} are zero and $-\omega_c$. Moreover, by construction, the eigenvalues of Q_{11} are the $2(N-1)$ eigenvalues of $\mathcal{Q}$ with strictly negative real part (see Proposition 9). □

C Electrical and simulation parameters

In this appendix, we provide the electrical and control parameters of Scenarios 1 and 2, described in Section 5.

Table 2: Electrical setup and line parameters

Converter and output filter parameters			
Input/Output DC voltage (V)		100/48	
DGU	Resistance $R_t(\Omega)$	Capacitance $C_t(mF)$	Inductance $L_t(mH)$
$\hat{\Sigma}^{DGU}_{[1]}$	0.2	2.2	1.8
$\hat{\Sigma}^{DGU}_{[2]}$	0.3	1.9	2.0
$\hat{\Sigma}^{DGU}_{[3]}$	0.1	1.7	2.2
$\hat{\Sigma}^{DGU}_{[4]}$	0.5	2.5	3.0
$\hat{\Sigma}^{DGU}_{[5]}$	0.4	2.0	1.3

Tie lines parameters		
Connected DGUs (i, j)	Resistance $R_s(\Omega)$	Inductance $L_s(\mu H)$
$(1, 3)$	0.07	2.1
$(2, 3)$	0.04	2.3
$(2, 4)$	0.08	1.8
$(3, 4)$	0.07	1
$(4, 5)$	0.05	2

Table 3: Primary and secondary control layer parameters.

Primary PnP control layer			
K_1	$[-2.134 \ -0.163 \ 13.553]$		
K_2	$[-0.869 \ -0.050 \ 48.285]$		
K_3	$[-0.480 \ -0.108 \ 30.673]$		
K_4	$[-6.990 \ -0.175 \ 102.960]$		
K_5	$[-0.101 \ -0.010 \ 16.393]$		
Secondary consensus layer			
Scenario 1		Scenario 2	
k_I	0.02	k_I	0.01

References

[1] A. Ipakchi and F. Albuyeh, "Grid of the future," *Power and Energy Magazine, IEEE*, vol. 7, no. 2, pp. 52–62, 2009.

[2] N. Hatziargyriou, H. Asano, R. Iravani, and C. Marnay, "Microgrids," *Power and Energy Magazine, IEEE*, vol. 5, no. 4, pp. 78–94, July 2007.

[3] R. Lasseter, "Microgrids," in *Power Engineering Society Winter Meeting, 2002. IEEE*, vol. 1, 2002, pp. 305–308 vol.1.

[4] J. M. Guerrero, M. Chandorkar, T.-L. Lee, and P. C. Loh, "Advanced control architectures for intelligent microgrids - part I: decentralized and hierarchical control," *IEEE Transactions on Industrial Electronics*, vol. 60, no. 4, pp. 1254–1262, 2013.

[5] J. M. Guerrero, P. C. Loh, T.-L. Lee, and M. Chandorkar, "Advanced control architectures for intelligent microgrids - part II: Power quality, energy storage, and ac/dc microgrids," *IEEE Transactions on Industrial Electronics*, vol. 60, no. 4, pp. 1263–1270, 2013.

[6] S. Riverso, F. Sarzo, and G. Ferrari-Trecate, "Plug-and-play voltage and frequency control of islanded microgrids with meshed topology," *IEEE Transactions on Smart Grid*, vol. 6, no. 3, pp. 1176–1184, May 2015.

[7] S. Bolognani and S. Zampieri, "A distributed control strategy for reactive power compensation in smart microgrids," *IEEE Transactions on Automatic Control*, vol. 58, no. 11, pp. 2818–2833, 2013.

[8] T. Dragicevic, X. Lu, J. Vasquez, and J. Guerrero, "Dc microgrids–part i: A review of control strategies and stabilization techniques," 2015.

[9] J. M. Guerrero, J. C. Vasquez, J. Matas, D. Vicuna, L. García, and M. Castilla, "Hierarchical control of droop-controlled ac and dc microgrids—a general approach toward standardization," *IEEE Transactions on Industrial Electronics*, vol. 58, no. 1, pp. 158–172, 2011.

[10] M. Tucci, S. Riverso, J. C. V. Quintero, J. M. Guerrero, and G. Ferrari-Trecate, "Voltage control of dc islanded microgrids: a decentralized scalable approach," in *54th IEEE Conference on Decision and Control*. IEEE, 2015, pp. 3149–3154.

[11] J. M. Guerrero, J. C. Vasquez, J. Matas, L. G. De Vicuña, and M. Castilla, "Hierarchical Control of Droop-Controlled AC and DC Microgrids — A General Approach Toward Standardization," *IEEE Transactions on Industrial Electronics*, vol. 58, no. 1, pp. 158–172, 2011.

[12] L. Meng, T. Dragicevic, J. Roldan-Perez, J. C. Vasquez, and J. M. Guerrero, "Modeling and sensitivity study of consensus algorithm-based distributed hierarchical control for dc microgrids," *IEEE Transactions on Smart Grid*, 2015. [Online]. Available: http://vbn.aau.dk/files/209623112/CA_based_DCMG_modeling_0409.pdf

[13] L. Meng, J. C. Vasquez, J. M. Guerrero, and T. Dragicevic, "Agent-based distributed hierarchical control of dc microgrid systems," *Electrimacs 2014*, pp. 281–286, 2014.

[14] A. Maknouninejad, Z. Qu, F. L. Lewis, and A. Davoudi, "Optimal, nonlinear, and distributed designs of droop controls for dc microgrids," *IEEE Transactions on Smart Grid*, vol. 5, no. 5, pp. 2508–2516, 2014.

[15] Q. Shafiee, T. Dragicevic, F. Andrade, J. C. Vasquez, and J. M. Guerrero, "Distributed consensus-based control of multiple dc-microgrids clusters," in *Industrial Electronics Society, IECON 2014-40th Annual Conference of the IEEE*. IEEE, 2014, pp. 2056–2062.

[16] J. Zhao and F. Dörfler, "Distributed control and optimization in dc microgrids," *Automatica*, vol. 61, pp. 18–26, 2015.

[17] M. Andreasson, D. V. Dimarogonas, H. Sandberg, and K. H. Johansson, "Control of mtdc transmission systems under local information," in *Decision and Control (CDC), 2014 IEEE 53rd Annual Conference on*. IEEE, 2014, pp. 1335–1340.

[18] J. Allmeling and W. Hammer, "Plecs-user manual," 2013.

[19] R. Grone, R. Merris, and V. S. Sunder, "The Laplacian spectrum of a graph," *SIAM Journal on Matrix Analysis and Applications*, vol. 11, no. 2, pp. 218–238, 1990.

[20] M. C. Pease, *Methods of matrix algebra*. Academic Press New York, 1965.

[21] A. Bensoussan and J.-L. Menaldi, "Difference equations on weighted graphs," *Journal of Convex Analysis*, vol. 12, no. 1, pp. 13–44, 2005.

[22] G. Ferrari-Trecate, A. Buffa, and M. Gati, "Analysis of coordination in multi-agent systems through partial difference equations," *IEEE Transactions on Automatic Control*, vol. 51, no. 6, pp. 1058–1063, June 2006.

[23] F. M. Callier and C. A. Desoer, *Linear system theory*. Springer Science & Business Media, 2012.

[24] R. Agaev and P. Chebotarev, "On the spectra of nonsymmetric laplacian matrices," *Linear Algebra and its Applications*, vol. 399, pp. 157–168, 2005.

[25] R. Diestel, *Graph theory*. Springer-Verlag Berlin and Heidelberg GmbH & amp, 2000.

[26] S. Lang, "Linear algebra. undergraduate texts in mathematics," 1987.

[27] Q. Shafiee, T. Dragičević, J. C. Vasquez, and J. M. Guerrero, "Modeling, Stability Analysis and Active Stabilization of Multiple DC-Microgrid Clusters," in *Proceedings of the IEEE International Energy Conference (ENERGYCON)*, Dubrovnik, Croatia, May 13-16, 2014, pp. 1284–1290.

[28] M. Babazadeh and H. Karimi, "A Robust Two-Degree-of-Freedom Control Strategy for an Islanded Microgrid," *IEEE Transactions on Power Delivery*, vol. 28, no. 3, pp. 1339–1347, 2013.

[29] V. Venkatasubramanian, H. Schattler, and J. Zaborszky, "Fast Time-Varying Phasor Analysis in the Balanced Three-Phase Large Electric Power System," *IEEE Transactions on Automatic Control*, vol. 40, no. 11, pp. 1975–1982, 1995.

[30] F. Dörfler and F. Bullo, "Kron reduction of graphs with applications to electrical networks," *IEEE Transactions on Circuits and Systems I: Regular Papers*, vol. 60, no. 1, pp. 150–163, 2013.

[31] M. Tucci, A. Floriduz, S. Riverso, and G. Ferrari-Trecate, "Kron reduction methods for plug-and-play control of ac islanded microgrids with arbitrary topology," *arXiv preprint arXiv:1510.07873*, 2015.

[32] R. Olfati-Saber and R. M. Murray, "Consensus problems in networks of agents with switching topology and time-delays," *IEEE Transactions on Automatic Control*, vol. 49, no. 9, pp. 1520–1533, 2004.

[33] Y. Hong and R. A. Horn, "The Jordan cononical form of a product of a hermitian and a positive semidefinite matrix," *Linear Algebra and Its Applications*, vol. 147, pp. 373–386, 1991.

[34] P.-A. Bliman and G. Ferrari-Trecate, "Average consensus problems in networks of agents with delayed communications," *Automatica*, vol. 44, no. 8, pp. 1985–1995, 2008.

[35] L. Meng, T. Dragicevic, J. M. Guerrero, and J. C. Vasquez, "Dynamic consensus algorithm based distributed global efficiency optimization of a droop controlled dc microgrid," in *Energy Conference (ENERGYCON), 2014 IEEE International*. IEEE, 2014, pp. 1276–1283.